ISSN 1648-4142 / eISSN 1648-3480

VILNIUS TECH
Vilnius Gediminas Technical University

TRANSPORT

2025
Volume 40
Issue 3
Pages 260–279
https://doi.org/10.3846/transport.2025.22868

Original Article

MULTI-BUS-LINE JOINT OPERATION STRATEGY OF OPTIMIZING BUS SPEED AND INTERSECTION SIGNAL PRIORITY TO MINIMIZE PASSENGERS WAITING TIME

Hong Guang ZHANG ✉, Ting Ting LIU, Yuan An LIU, Xiang LI

School of Electronic Engineering, Beijing Key Laboratory of Work Safety Intelligent Monitoring, Beijing University of Posts and Telecommunications, Beijing, China

Highlights:

- intelligent bus system model with multi-bus-lines and time-varying passenger flow;
- jointly optimize bus speed on dedicated bus lanes and intersection signal priority;
- real-time rescheduling framework by using TSSA;
- simulate the multi-pattern search foraging of salp swarm to enrich search behaviours.

Article History:

- submitted 8 April 2022;
- resubmitted 3 October 2022, 27 December 2022;
- accepted 2 April 2023.

Abstract. The rapid increase in the number of vehicles reduces the efficiency of transportation networks in modern big cities. Thus, minimizing passengers waiting time by bus has become an inevitable approach. Through intelligent bus systems and Dedicated Bus Lanes (DBLs), jointly optimizing bus speed and intersection signal priority has become a feasible research objective for multi-bus-lines. Moreover, the length of Beijing (China) DBLs will be 1020 km in 2022. Considering the requirements of the Beijing Bus Group, a problem model is formulated, including multi-bus-lines, time-varying passenger flow, bus-speed-control only on DBLs, and intersection signal control. In this study, the real-time framework of the multi-bus-line joint operation strategy with the Transformable Salp Swarm Algorithm (TSSA) is proposed. Moreover, the small optimization interval effectively reduces the impact of bus-speed-control inaccuracy and the errors between the joint optimization scheme and actual operation states. In the real-time framework, only the speed of the bus traveling on DBLs could be guided in the form of real-number speed, and this bus-speed scheme is safe. Additionally, the strategy could compensate for the travel time in the non-priority direction after buses pass through intersections, and this is effective to avoid traffic congestion. As the online optimization algorithm, TSSA simulates the grouping activity of salp swarms. Based on actual data from Beijing Bus Group, 6 test problems are constructed, and the joint operation strategy outperforms others.

Keywords: joint operation strategy, multi-bus-line, time-varying passenger flow, speed guidance on dedicated bus lane, traffic signal priority.

✉ Corresponding author. E-mail: *hongguang-zhang@bupt.edu.cn*

Notations

AHDR – average headway deviation ratio;
AVL – automatic vehicle location;
AWTP – average waiting time of passengers;
CAV – connected and autonomous vehicle;
CSP – conditional signal priority;
CV – connected vehicle;
DBL – dedicated bus lane;
DVRP – dynamic vehicle routing problem;
FIFS – 1st-in-1st-service;
ICT – information and communication technologies;
non-DBL – non-dedicated bus lane;
MBGA – memory-based genetic algorithm;
PACT – person-based adaptive traffic signal control method with cooperative transit signal priority;
SHC – sequential hill climbing;
SSA – salp swarm algorithm;
TSP – traffic signal priority;
TSSA – transformable SSA;
V2I – vehicle to infrastructure;
V2V – vehicle to vehicle.

1. Introduction

In recent years, the area of modern big cities has doubled, and the number of vehicles has increased rapidly. As a result, urban traffic congestion becomes prominent, and road traffic efficiency is seriously disturbed. For instance, congestion costs in the US increased from 1982 to 2011 (Schrank *et al.* 2012). The congestion invoice for the cost of extra time and fuel in 498 urban areas was (all values in constant 2011 dollars): $24 billion in 1982, $94 billion in 2000, and $121 billion in 2011 (Schrank *et al.* 2012).

Public transportation has played a central role in the urban transportation system. From 1982 to 2005, the savings on congestion costs caused by public transport services increased by nearly 131% in the US (Moreira-Matias *et al.* 2015). This increase was 10% between 2005 and 2011 (Moreira-Matias *et al.* 2015). Moreover, the bus is the primary travel mode of public transportation. The service level of the bus system directly affects the travel choice of urban residents. Thus, minimizing passengers waiting time by bus has become an inevitable approach to improve the efficiency of ground transportation networks.

The long waiting time of passengers is an important reason for the deterioration of bus service. In Beijing (China), emerging wireless communication technology and infrastructure construction could significantly improve the quality of bus service. Detailed explanations are as follows:

- ***real-time information collection***: with the large-scale applications of ICT, intelligent bus systems based on CVs, AVL, V2V, and V2I have been widely deployed in modern big cities (Gong *et al.* 2019). Based on these infrastructures, intelligent bus systems collect real-time information on traffic congestion, vehicle information, and passenger flow in many cities, such as Beijing (Shang *et al.* 2019), Shanghai (Shan *et al.* 2019), Melbourne (Mazloumi *et al.* 2010), and London (Hounsell *et al.* 2012), and so on;
- ***speed guidance on DBLs***: as the most fundamental infrastructure, DBLs are widely used and have played an essential role in reducing traffic congestion. It is worth mentioning that the length of Beijing DBLs will be 1020 km in 2022. As shown in Figure 1, buses on DBLs could realize speed guidance according to the control instructions from the traffic management center. The reason is that buses are not affected by private vehicles on DBLs. Otherwise, on non-DBLs, buses and private vehicles drive together and affect each other;
- ***intersection signal control systems***: the traffic management center also controls intersection signal lights to make buses pass through intersections, and this improves the priority of buses at the intersection.

Generally, through intelligent bus systems and DBLs, jointly optimizing bus speed and intersection signal priority for multi-bus-lines has become a feasible research objective to minimize passengers waiting time. This is good to make more passengers travel by buses instead of private vehicles, thus reducing congestion costs in the metropolis.

To ensure the operation quality of bus lines, many researchers have studied bus scheduling or control strategies, such as holding strategy (Asgharzadeh, Shafahi 2017; He *et al.* 2020), stop-skipping (Zhao *et al.* 2021), short turning (Gkiotsalitis *et al.* 2019; Tian *et al.* 2022), overtaking (Wu *et al.* 2017), passenger boarding limit (Zhao *et al.* 2016; Saw *et al.* 2020), speed control and guidance (Daganzo, Pilachowski 2011; Varga *et al.* 2018; He *et al.* 2019; Dadashzadeh, Ergun 2019; Bian *et al.* 2020; Deng *et al.* 2020; Ampountolas, Kring 2021), intersection signal priority (Li *et al.* 2011, 2016; Ghanim, Abu-Lebdeh 2015; Jia *et al.* 2019; Yang *et al.* 2019; Anderson, Daganzo 2020; Hao *et al.* 2021; Lee, Wang 2022), joint operation strategy (Wu *et al.* 2016; Li *et al.* 2019; Zhang *et al.* 2022; Wu *et al.* 2022; Xu *et al.* 2019; Colombaroni *et al.* 2020; Zimmermann *et al.* 2021; Zhao *et al.* 2022), and so on. Due to intelligent bus systems and DBLs, joint operation strategy has become a research focus. Most joint operation strategies combine signal priority, bus holding, and speed control. However, the holding strategy means passengers

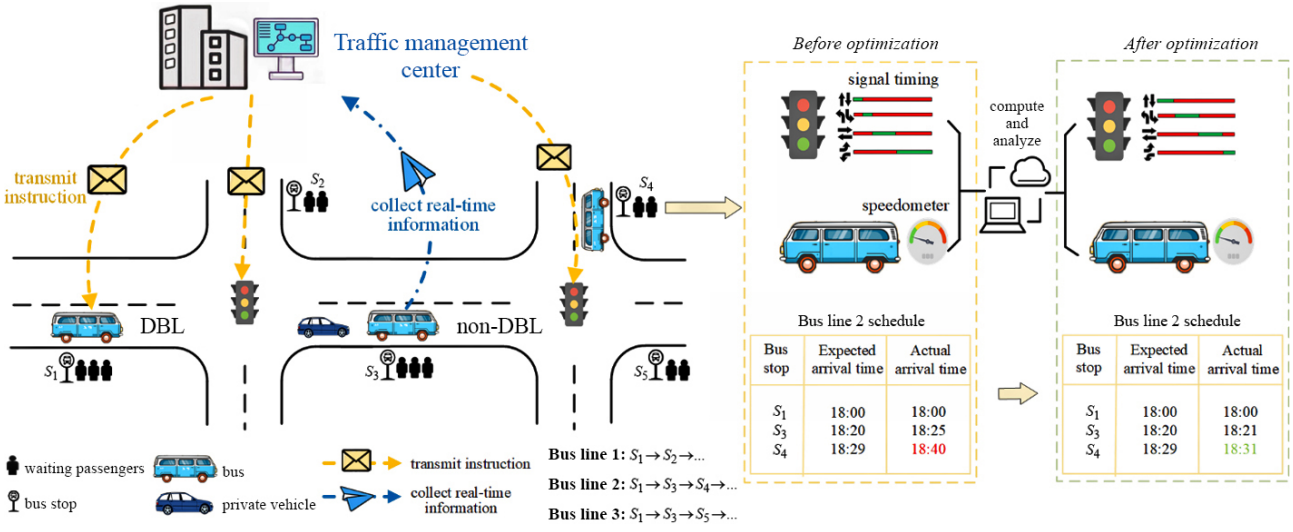

Figure 1. Research problem and scenario

need to wait for extra time at stops. From a passenger perspective, compared with travel time, the long dwell time usually reduces passenger satisfaction. On the other hand, some previous studies mainly focused on a single bus line. However, there are often overlapping sections of multi-bus-lines (i.e., multi-bus-lines pass through the same section) in the real transportation network. Different buses interact in these overlapping sections, which may degrade the performance of the single-line optimization strategy. Therefore, it is necessary to study the optimization strategy of multi-bus-line.

To address this problem in Figure 1, a case study is conducted in Beijing involving 12 bus lines and 242 stops. A multi-bus-line joint operation strategy of optimizing bus speed and intersection signal priority is proposed. The main contributions include:

- ***intelligent bus system model considering real factors***: previous studies rarely considered the discontinuity of DBLs. An intelligent bus system model is designed considering real factors such as discontinuous DBLs and time-varying passenger flow to improve the practicability of the model. Then, the passengers waiting time on multi-bus-lines is formulated, and the optimization goal is to minimize the passengers waiting time;
- ***joint operation strategy***: the real-time optimization framework based on rolling optimization intervals is designed. Based on the intelligent bus system, the constraints of speed and signals to jointly optimize bus speed and intersection signal priority are introduced. Moreover, this strategy provides a solution for handling signal conflicts and reducing non-priority phase delay at multi-bus-line intersections;
- ***TSSA***: an online optimization algorithm named TSSA is developed. TSSA simulates the mechanism of asexual and sexual reproduction of salp swarm to balance exploitation search effort and exploration search effort. Then, by simulating the multi-pattern search foraging of salp swarm, the chain and linear patterns are innovatively used for exploitation search, and the cluster and helical patterns are used for exploration search. This effectively improves the search performance of TSSA. The case study results imply that the joint operation strategy outperforms others.

The article is organized as follows:

- current section 1 is an introduction;
- section 2 presents a brief overview of related works;
- section 3 introduces the description of intelligent bus systems and model formulation;
- section 5 introduces the multi-bus-line joint operation strategy;
- section 5 describes the case study in Beijing Bus Group;
- last section 6 summarizes conclusions and future work.

2. Literature review

In intelligent bus systems, speed control and guidance, intersection signal priority, and joint operation strategy are strongly related to the research problem. The latest research is reviewed as follows.

2.1. Speed control and guidance

The development of CVs, AVL, V2V, and V2I provides new opportunities for realizing speed control and guidance. The recent research about speed control and guidance has been proposed to guide drivers to adjust bus speed, avoid unnecessary parking, and reduce bus delays. Daganzo & Pilachowski (2011) proposed an adaptive control scheme that continuously adjusts the bus cruising speed based on a cooperative 2-way-looking strategy. This scheme could yield regular headways with faster bus travel. Varga *et al.* (2018) presented a selected rolling horizon control scheme to choose proper speed profiles for the bus such that it keeps the timetable schedule and achieves desired headways. Bian *et al.* (2020) proposed an optimization-based speed control method. This method focused on one-way transit corridors and considered the phenomenon of bus queuing. However, none of the above schemes analyses the realizability of vehicle speed control in practice. When the road is crowded, with the influence of the complex traffic environment, the bus may not travel at the recommended or optimal speed.

In many cases, only the speed of the bus traveling on DBLs can be adjusted. He *et al.* (2019) studied a bus speed adjustment strategy by looking at multiple critical time points on DBLs. This method stabilized a strongly unstable bus line and shortened passengers' waiting and riding time. Dadashzadeh & Ergun (2019) provided a combination of variable speed limits and ramp metering strategies. This method effectively reduced delay times on the Metrobus system. Deng *et al.* (2020) proposed a real-time bus-speed-control method. They modelled signal intersection delay and heterogeneous roadway, and considered other common variables such as passenger boarding/alighting times. Ampountolas & Kring (2021) defined a platoon of buses operating in the same transit line as leader-follower dyads. The driver of the following bus could observe the position and speed of the leading bus. The leader transmits information to control the speed of the follower to eliminate bunching.

2.2. TSP

TSP is effective to improve the efficiency of public transport services. Li *et al.* (2011) provided an architecture overview of adaptive TSP systems. Then, they proposed an adaptive TSP optimization model to minimize the weighted sum of transit vehicle delays and other traffic delays. This means that signal timing could be adjusted to make buses with higher priorities over private vehicles passing through intersections. Ghanim & Abu-Lebdeh (2015) proposed a real-time optimization method of dynamic TSP and used a genetic algorithm and artificial neural network method to address this problem. Considering the 3 priority strategies of green extension, red truncation, and phase insertion, Li *et al.* (2016) developed a dual objective optimization method of transit signal priority to minimize passenger delay and bus-schedule deviation. To improve intersections' traffic efficiency and environmental

benefits, a multi-objective optimization method for intersection signal timing was proposed by Jia *et al.* (2019). They considered the optimization goals, such as delay per capita, vehicle emission, and intersection capacity. Yang *et al.* (2019) proposed a TSP algorithm using CV information for multimodal traffic control. Anderson & Daganzo (2020) evaluated a CSP, in which the bus sends priority requests only when the request improves reliability. They analysed 3 forms of driver control, and the results showed that CSP greatly reduced the number of priority requests, thereby improving reliability. Hao *et al.* (2021) proposed a bus signal priority model with the consideration of the proportion of the arriving traffic at the intersection between bus and non-bus. And they introduced the phase clearance reliability of the bus and non-bus phases in the model. Lee & Wang (2022) proposed a PACT system. PACT performed signal optimization through the rolling horizon procedure to reduce bus delays.

2.3. Joint operation strategy

Most existing TSP studies usually assume that bus speed is fixed as a constant. Recently, due to the ICT applications in intelligent bus systems, more researchers have proposed joint operation strategies to improve bus punctuality. Most of them are based on the combinations of TSP, speed control and guidance, and holding strategy. Wu *et al.* (2016) proposed a bus operation control approach with speed control and holding control strategies to minimize the total cost of bus signal delay, bus holding delay, bus travel delay, and acceleration cost. By combining the bus holding strategy with the operating speed control strategy, Li *et al.* (2019) studied a robust dynamic control mechanism. This approach could reduce the bus bunching phenomenon. Zhang *et al.* (2022) combined the boarding limit strategy and bus holding strategy to improve bus service and minimize bus headway. Wu *et al.* (2022) designed a new flexible multi-type bus shuttle system, integrating ride-matching and flexible timetabling. To improve the flexibility of bus schedules, they introduced stop-skipping, speed adjustment and bus holding strategies. Xu *et al.* (2019) combined traffic signal optimization with vehicle speed control for CAVs, which may improve both transportation efficiency and fuel economy. Colombaroni *et al.* (2020) developed a simulation-optimization method for signal synchronization with bus priority and driver speed advisory to CVs. Simulation results implied that offline signal optimization and online signal priority reduce the travel times and delays of buses. Zimmermann *et al.* (2021) jointly optimized bus holding, speed guidance, and multiple traffic signals for regularizing bus headways. They gave a bus trajectory model, formulated a multi-objective function, and finally solved it through a lexicographic method. Zhao *et al.* (2022) used speed control and green light extension strategies to dynamically optimize bus scheduling on overlapping sections.

However, the above research usually assumes that all buses travel on DBLs or in a 100% CAVs environment. In the real transportation system, discontinuous DBLs increase the difficulty of speed control. Moreover, there are usually overlapping sections of multi-bus-lines, making the optimization strategy more complicated.

3. Intelligent bus system and model formulation

With CVs, AVL, V2I, and V2V continuously emerging, waiting time and improving bus punctuality are feasible by optimizing bus speed and intersection signal priority in intelligent bus systems. In this section, the multi-bus-line joint operation problem is formulated to minimize passengers waiting time. Mathematically speaking, this optimization objective depends on adjusting each bus speed and intersection signal control in multi-bus-lines.

3.1. Description of intelligent bus system

On assumptions. In this model, intelligent bus systems make full use of CVs, AVL, V2I, and V2V technologies. Moreover, all buses and intersections are the connected devices of the traffic management center in intelligent bus systems (Miller 2008; Kaiwartya *et al.* 2016). The traffic management center could collect all information in real-time, adjust bus speed, and control intersection signal priority.

On multi-bus-lines. There are multi-bus-lines with fixed routes that include different stops and intersections. And there are many buses in each bus line. For instance, in bus line 601, there are 20 buses to be scheduled every day. The start time of all buses is 6:00 AM, and the departure interval is 15 min. Then, the bus departure time of the nth bus in the ith bus line D_{i-n} is 6:00 AM $+\left(n-1\right)\cdot$15 min. Note that the headway of adjacent buses may not be equal to 15 min because of various uncertain times (e.g., uncertain time that passengers get on/off).

3.1.1. Bus speed model

Benefits of speed guidance. The travel speed of one bus determines its travel time on the road segment and the time to reach the intersection, which further affects the traffic of the bus at intersections and the time to reach stops. Therefore, effective speed guidance could reduce the waiting time of passengers.

The feasibility of speed guidance. The development of CVs has significantly increased driving accuracy, reduced the high uncertainty related to manual driving, and improved the efficiency of city traffic. The Internet of vehicles provides technical support to obtain the actual positions and speeds of vehicles in real-time. Thus, it becomes possible to accurately control the vehicle speed based on CVs, AVL, V2I, and V2V technologies. Moreover, the small optimization interval ensures the feasibility of speed guidance, which will be described in Section 4.1.

From a bus-speed-control perspective, only buses on DBLs could be managed to realize speed guidance by the traffic management center. There are 2 different scenarios:

- ***on DBLs***: when buses travel on DBLs, they are not affected by private vehicles. Thus, the traffic management center transmits control instructions to buses on DBLs to realize speed guidance. Then, these buses could accelerate or decelerate as needed. Besides, one bus speed on different DBLs is guided by different control instructions in real-time. When the nth bus of the ith line travels on the road section R_m (road section between the mth node and the $(m+1)$th node in the ith bus line) of DBL, its speed is V_{i-n}^m. In practice, bus speed should be constrained by the maximum speed $V_{\max}^m$ and the minimum speed $V_{\min}^m$ of V_{i-n}^m. In this model, $V_{\max}^m$ and $V_{\min}^m$ are obtained from the real statistical data on R_m;
- ***on non-DBLs***: when buses travel on non-DBLs, they are affected by traffic congestion. Considering traffic safety, it is difficult to realize speed control. Thus, the traffic management center does not control bus speed on non-DBLs in this model.

3.1.2. Intersection signal model

Introduction of standard ring-and-barrier. The traffic signal timing manual (Koonce *et al.* 2008) is referenced to illustrate a typical ring-and-barrier model. Figure 2a shows a typical 4-leg, 2-lane (in each direction) intersection. There is a left-turning lane and a through /right-turning lane in each intersection direction. Figure 2b demonstrates a standard ring-and-barrier signal control design (Koonce *et al.* 2008). One intersection includes 8 phases (i.e., phases 1...8) after combining the through and right turn movements for the same direction. The sequence of phases is shown as they occur in time, proceeding from left to right.

The signal timing of the ring-and-barrier model. The signal timing of the ring-and-barrier model in a signal period is explained as follows. It is worth noting that the traffic management center could adjust these phase times by using real values. Figure 3 presents the signal control design used in this model. The phase-switching procedure is phases 1&5 (east–west left) → phases 2&6 (east–west through) → phases 3&7 (north–south left) → phases 4&8 (north–south through). The phase time is the sum of the green and yellow light times. For example, the uth phase time p_u is given by:

$$p_u = g_u + y_u, \tag{1}$$

where: p_u is the uth phase time of a signal; g_u is green light time; y_u is yellow light time that is equal to 3 s in this article.

Therefore, the sum of all phase times at an intersection is a signal period, given by:

$$C_{light} = \sum_{u=1}^{h} p_u, \tag{2}$$

where: C_{light} is the signal period that is equal to 150 s in this article; h is the total number of phases.

In Figure 3, there are 4 phases. Thus, h = 4. Note that, according to the historical traffic flow statistics, the traffic management center could compute the relatively ideal phase times of an intersection signal.

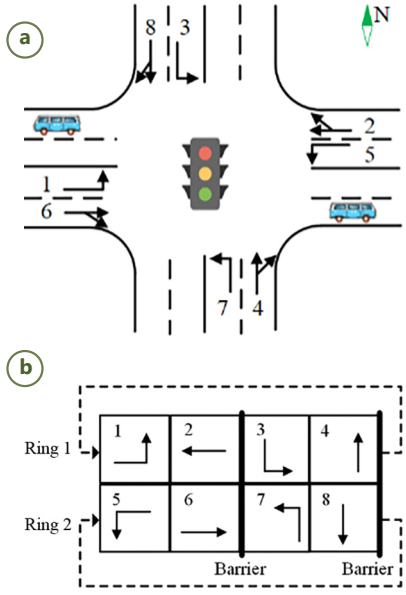

Figure 2. Illustration of the phases of one intersection and its phase switching rules:
(a) – schematic diagram of intersection;
(b) – standard ring-and-barrier diagram

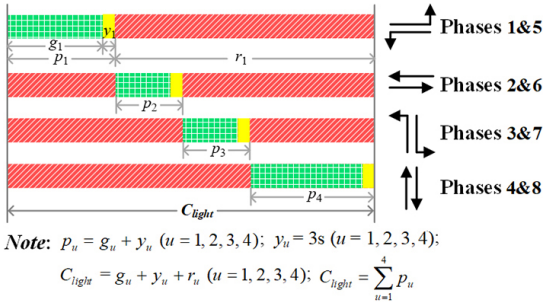

Figure 3. Illustration of the phase switching and timing scheme

Then, these relatively ideal times are usually used as the conventional values of the phase times of an intersection signal. Meanwhile, to avoid the long waiting time for pedestrians, the signal light time should be constrained by:

$$\begin{cases} C_{light} = g_u + y_u + r_u; \\ g_u \geq t_{\min}^g; \\ r_u \leq t_{\max}^r, \end{cases} \tag{3}$$

where: r_u is the red light time; $t_{\min}^g$ is the minimum green light time; $t_{\max}^r$ the maximum red light time.

Generally, p_u is optimized to improve bus priority to pass through intersections.

3.2. Model formulation

This model considers the scenario that the nth bus in the ith bus line arrives at the zth stop. That is to say, before the zth stop, there are $(z-1)$ stops, f intersections, and $(f+z-1)$ road sections in the ith bus line. Then, the time of arriving at the zth stop for the nth bus in the ith bus line is given by:

$$T_{i-n}^{z} = T_{dep} + T_{road} + T_{int} + T_{stop} = D_{i-n} + \sum_{m=1}^{f+z-1}\left(\frac{d\left(N_i^m, N_i^{m+1}\right)}{V_{i-n}^m}\right) + \sum_{q=1}^{f} T_{int}\left(i, n, q\right) + \sum_{k=1}^{z-1} t_{board} \cdot \max\left(\beta_i^k\left(t\right) \cdot O_{i-n}^k, B_{i-n}^k\right), \quad (4)$$

where: T_{i-n}^{z} is the time of the nth bus in the ith bus line arrives at the zth stop; T_{dep} is the departure time of the nth bus; T_{road} is the time sum of passing through $\left(f+z-1\right)$ road sections; T_{int} is the time sum of passing through f intersections; T_{stop} is the time sum of passing through $(z-1)$ stops; N_i^m is the mth node in the ith bus line (N_i^m may be a stop or an intersection); D_{i-n} is the nth bus departure time in the ith bus line; V_{i-n}^m is the real speed of the nth bus in the ith bus line when passing through the mth section road.

There are explanations:

- $d\left(N_i^m, N_i^{m+1}\right)$ returns the distance between N_i^m and N_i^{m+1}. In real scenarios, these data could be obtained by using map queries (such as *Google Maps* and so on). According to these data and real bus locations, the traffic management center could select one rational speed for each bus;
- $T_{int}\left(i, n, q\right)$ returns the time of passing through the qth intersection I_q of nth-bus in the ith bus line. If the phase of the bus driving direction is green, $T_{int}\left(i, n, q\right) = 0$. Otherwise, $T_{int}\left(i, n, q\right)$ is equal to the real waiting time. In intelligent bus systems, T_{int} is obtained according to the phase duration of these f traffic lights;
- at the kth bus stop S_k, the waiting time of one bus $t_{board} \cdot \max\left(\beta_i^k\left(t\right) \cdot O_{i-n}^k, B_{i-n}^k\right)$ is equal to the product of the maximum number of passengers who get on/off this bus and t_{board}. t_{board} is the time for one passenger to get on/off the bus. In this article, $t_{board} = 2\,\text{s}$. $\beta_i^k\left(t\right)$ is the passenger drop-off rate function of bus stop S_k in the ith bus line at time t, which is the ratio of the number of disembarking passengers to the number of passengers on board (Luo *et al.* 2019). When the number of passengers on board is 0, $\beta_i^k\left(t\right) = 0$. O_{i-n}^k is the number of passengers on the nth bus of the ith bus line, before it arrives at bus stop S_k. $\beta_i^k\left(t\right) \cdot O_{i-n}^k$ is the number of passengers who get off this bus. B_{i-n}^k is the number of passengers boarding at bus stop S_k for the nth bus of the ith bus line. $\max\left(\beta_i^k\left(t\right) \cdot O_{i-n}^k, B_{i-n}^k\right)$ is the maximum number of passengers who get on/off this bus.

As shown in Figure 4, the passenger flow is time-varying in this model. Thus, the number of passengers arriving at different times is different, which corresponds to the time for one passenger to get on/off the bus $t_{board} \cdot \max\left(\beta_i^k\left(t\right) \cdot O_{i-n}^k, B_{i-n}^k\right)$. For instance, the passenger flow in the morning is different from the passenger flow in the afternoon, as shown in Equation (7) and Figure 4. These are consistent with the real application scenario of the traffic management center. However, this increases the complexity of the optimization problems. The detailed explanations of $t_{board} \cdot \max\left(\beta_i^k\left(t\right) \cdot O_{i-n}^k, B_{i-n}^k\right)$ are as follows:

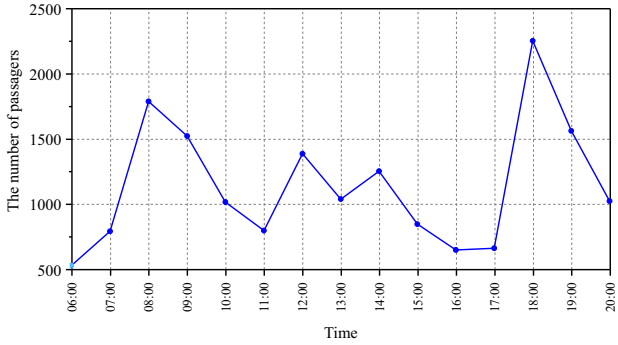

Figure 4. The number of passengers arriving at stops in one day

- in Equation (5): C is the maximum passenger capacity of a bus; W_{i-n}^k is the number of passengers waiting at bus stop S_k for the nth bus of the ith bus line; the number of passengers boarding at stop S_k is the minimum value between the remaining passenger capacity of the nth bus and the number of passengers waiting at stop S_k;
- the number of passengers on the nth bus when it arrives at stop S_k is obtained by using Equation (6); the number of passengers is the sum of the number of passengers when the bus arrives at the previous stop and the number of people getting on and off at the previous stop;
- Equation (7) shows that passenger flow is time-varying; $\lambda_i^k\left(t\right)$ is the passenger arrival rate function of bus stop S_k in the ith bus line at time t (Luo *et al.* 2019); $L_{i-(n-1)}^k$ is the number of passengers who don't board the $(n-1)$ th bus at bus stop S_k in the ith bus line; the number of passengers waiting at stop S_k is the sum of the number of passengers not boarding the $(n-1)$th bus and the number of passengers arriving within the time interval between the $(n-1)$th bus and the nth bus arriving at stop S_k;
- in Equation (8), the number of passengers who do not board the $(n-1)$th bus at stop S_k is the difference between the number of passengers waiting at stop S_k and the number of passengers boarding the $(n-1)$th bus.

$$B_{i-n}^k = \min\left(C - O_{i-n}^k + \beta_i^k\left(t\right) \cdot O_{i-n}^k, W_{i-n}^k\right); \quad (5)$$

$$O_{i-n}^k = \begin{cases} 0, & k = 1; \\ O_{i-n}^{k-1} + B_{i-n}^{k-1} - \beta_i^{k-1}\left(t\right) \cdot O_{i-n}^{k-1}, & \text{otherwise}; \end{cases} \quad (6)$$

$$W_{i-n}^k = \begin{cases} \int_{D_{i-n}}^{T_{i-n}^k} \lambda_i^k\left(t\right) \mathrm{d}t, & n = 1; \\ \int_{D_{i-n}}^{T_{i-n}^k} \lambda_i^k\left(t\right) \mathrm{d}t + L_{i-(n-1)}^k, & \text{otherwise}; \end{cases} \quad (7)$$

$$L_{i-(n-1)}^k = W_{i-(n-1)}^k - B_{i-(n-1)}^k. \quad (8)$$

Generally, the optimization objective is to minimize the waiting time of all passengers that is given by:

$$\underset{p_u, V_{i-n}^m}{\text{minimize}} \left(\sum_{i=1}^{N_l} \sum_{k=1}^{N_{si}-1} \sum_{n=1}^{N_{bi}} w_{i-n}^k\right); \quad (9)$$

$$W_{i-n}^{k}=\begin{cases}\int_{D_{i-n}}^{T_{i-n}^{k}}\lambda_{i}^{k}(t)\cdot\left(T_{i-n}^{k}-t\right)\mathrm{d}t, & n=1;\\ \int_{T_{i-(n-1)}^{k}}^{T_{i-n}^{k}}\lambda_{i}^{k}(t)\cdot\left(T_{i-n}^{k}-t\right)\mathrm{d}t+L_{i-(n-1)}^{k}\cdot\left(T_{i-n}^{k}-T_{i-(n-1)}^{k}\right), & n>1,\end{cases} \tag{10}$$

where: W_{i-n}^{k} is the total waiting time of passengers in the time interval between the (n – 1)th bus and the nth bus arriving at stop S_k; N_l is the number of lines; N_{si} is the number of stops in the ith bus line; N_{bi} is the number of buses in the ith bus line.

4. Multi-bus-line joint operation strategy

4.1. Framework

From a rolling-optimization-interval perspective, the multi-bus-line joint operation strategy is an online optimization strategy performed in each optimization interval. Figure 5 explains the real-time framework of the multi-bus-line joint operation strategy. Specifically, there are *n_max* optimization intervals in one day's bus operation time. The traffic management center executes TSSA to obtain the best solution based on the real-time information collected from buses and intersections. The decision variable of TSSA includes bus-speed-control and signal timing (Sections 4.2.1 and 4.2.2). Through multiple iterations and repairing the infeasible solution (Section 4.2.3), the optimal solution of TSSA is obtained (Section 4.3). According to the best solution, the traffic management center transmits control instructions to buses and intersections at the beginning of each optimization interval. Then, the bus adjusts its speed on the next DBLs according to the received speed guidance suggestions. The intersection adjusts the signal timing in corresponding signal periods and compensates for the non-priority phase when no bus passes, reducing the traffic congestion of private vehicles. In general, the traffic management center continuously repeats the previous process.

In real scenarios, the difficulty of speed control is greater than that of signal light control. However, a small optimization interval (i.e., 150 s) could reduce the influence of uncertain factors on speed guidance. For example, if the actual operating speed deviates from the expected speed, this deviation can be adjusted in time in the next interval through signal control and speed guidance to reduce the impact of inaccurate speed control.

4.2. Development of joint optimization scheme

4.2.1. Decision variables

In Equations (4) and (10), the waiting time of passengers is affected by the departure time of the bus T_{dep}, the traveling time of the bus on the road T_{road}, the waiting time of the bus at the intersection T_{int}, and the time required for passengers to get on and off T_{stop}. For buses with fixed departures, it is difficult to control T_{dep} and T_{stop}. Therefore, this scheme optimizes T_{road} and T_{int} to reduce the waiting time of passengers. These 2 times are affected by bus speed and light timing. According to the above analysis, the decision variable is designed.

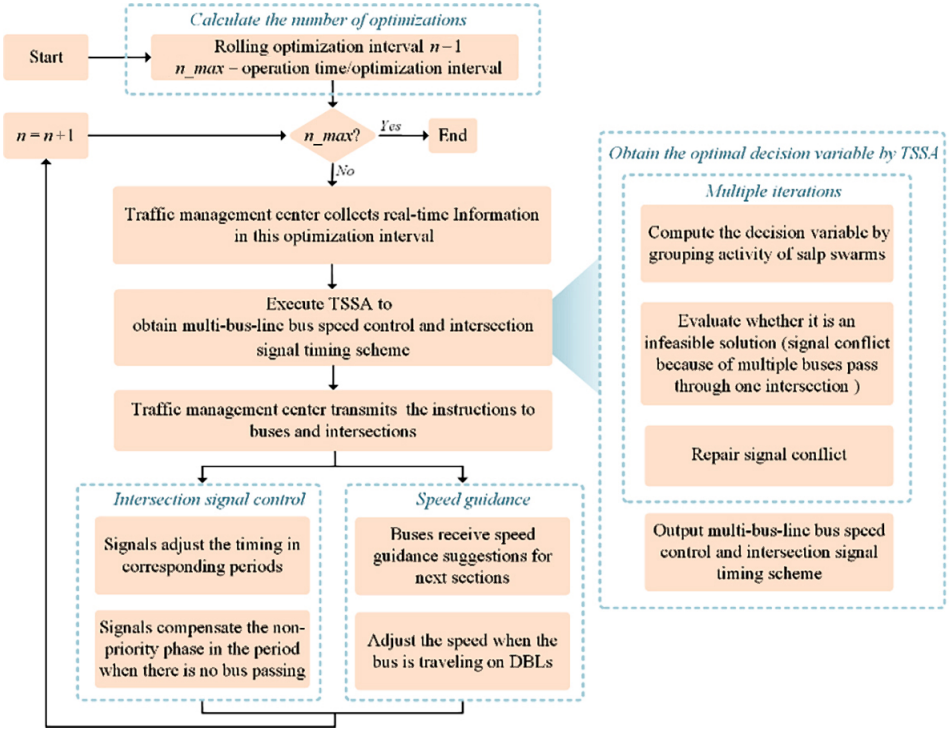

Figure 5. The real-time framework of multi-bus-line joint operation strategy

The decision variable is the real-number sequence. Quite simply, the real-number decision variable is the best solution of TSSA in every optimization interval. According to the decision variable, the speed of buses on DBLs and the signal timing of each intersection could be obtained. Then, the traffic management center transmits control instructions to buses and intersections. Note that the decision variable includes 2 parts:

- bus speed on DBLs V_{i-n}^{m};
- intersection signal timing P_u.

As shown in Figure 6, there are 4 combinations for the stop–intersection section:

- the road section between stop and intersection (like R_1);
- the road section between 2 adjacent intersections (like R_2);
- the road section between intersection and stop (like R_3);
- the road section between 2 adjacent stops (like R_4).

Considering the 1st and 2nd combinations, the code sequence is composed of the mid-block speed and 4 typical phase times when the bus arrives at the intersection (like *Code1* and *Code2*). For example, *Code1* includes the bus speed V_{i-n}^{1} on section R_1 and the signal timing $p_1 \ldots p_4$ of intersection I_1. In respect of the 3rd and 4th combinations, the downstream of the road section is not an intersection. The code sequence consists of the mid-block speed (like *Code3* and *Code4*). For example, *Code3* is the bus speed V_{i-n}^{3} on section R_3. Note that only the speed of the bus traveling on DBLs could be guided.

4.2.2. Speed and signal constraints of joint optimization

Speed and signal should be further constrained when the optimal decision variables are computed using TSSA.

Speed constraint. From a bus-speed-control perspective, this strategy only adjusts the bus speed V_{i-n}^{m} on DBLs. Detailed explanations are as follows:

- due to the influence of private vehicle driving, realizing speed guidance for the buses on non-DBL is difficult. Therefore, the bus speed on non-DBL cannot be controlled;
- considering road sections with DBLs, there is almost no road congestion. This means buses could choose the proper speed according to instructions of the traffic management center;
- when planning a bus line, designers consider many objectives, such as passenger safety, minimizing passengers waiting time, ensuring bus punctuality rate, and so on. Then, they could obtain a reasonable plan for this bus line that includes the bus-speed baseline of each DBL. Thus, the proper speed range is also obtained based on the bus-speed baseline of each DBL.

As discussed in Section 3.1.1, bus speed on DBLs is constrained by the minimum and maximum speeds, which is:

$$V_{\min}^{m} \le V_{i-n}^{m} \le V_{\max}^{m}. \tag{11}$$

Signal constraint. From an intersection-signal-control perspective, the strategy adjusts the signal timing p_u to improve the priority of buses passing through the intersection. Signal control should be constrained to reduce the impact of adjusting signal timing on vehicles and pedestrians in non-priority directions. Intersection signal optimal control considers green, yellow, and red light times. The constraint of each phase is given by:

$$t_{\min}^{g} + y_u \le p_u \le C_{light} - \left(h-1\right)\cdot\left(t_{\min}^{g} + y_u\right), \tag{12}$$

where: y_u is yellow light time that is equal to 3 s; h is the total number of phases; C_{light} is the signal period.

In a signal period C_{light}, $t_{min}^{g} + y_u$ is the minimum value of each p_u. Note that, $\left(h-1\right)\cdot\left(t_{min}^{g} + y_u\right)$ is the sum of the minimum values of other phases. $C_{light} - \left(h-1\right)\cdot\left(t_{min}^{g} + y_u\right)$ is the maximum value of each p_u, which is obtained by subtracting the sum of other phase minimum values from a signal period C_{light}. In addition, another constraint is introduced, that is, a signal cannot accept 2 timing schemes in one signal period.

4.2.3. Multi-bus-line optimization

The goal is to minimize passengers waiting time for multi-bus-lines. Therefore, when TSSA is used to obtain the optimal decision variable (i.e., bus speed on DBLs and intersection signal timing like Figure 6), the code sequence of all departing buses on all lines is computed in the present optimization interval.

Conflict of signal timing for multi-bus-lines. There are often overlapping sections of multi-bus-lines. When multiple buses pass through one intersection in the same signal period, their timing schemes for that signal may be inconsistent. As shown in Figure 7, the intersection's coding requirements are different when the buses A_{1-n} and A_{2-n} pass through intersection I_1. Thus, this is not a feasible solution. The conflict is explained as follows.

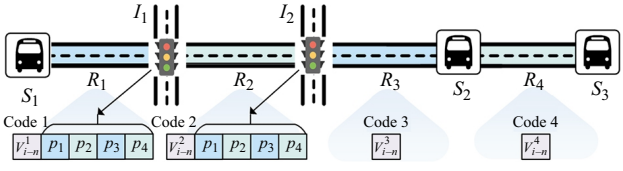

Figure 6. The real-number decision variable

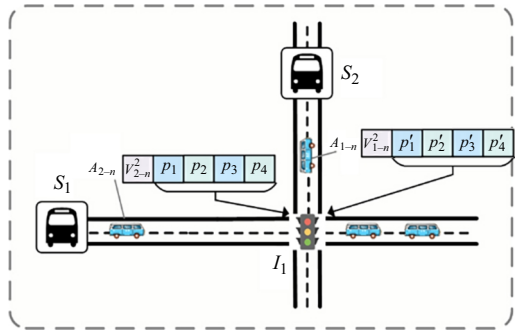

Figure 7. Multiple buses pass through one intersection in the same signal period

1st, the period number of the signal when the bus arrives at the intersection could be predicted by:

$$\varepsilon = floor\left(\frac{\frac{d\left(N_i^m, N_i^{m+1}\right)}{V_{i-n}^m} + t_{entry}}{C_{light}}\right) + 1, \quad (13)$$

where: $floor()$ is the round function toward negative infinity; $d\left(N_i^m, N_i^{m+1}\right)$ is the mth road section length; V_{i-n}^m is travel speed; C_{light} is the signal period; C_{entry} is the time that the bus enters this road section.

2nd, if A_{1-n} and A_{2-n} arrive at the intersection I_1 in different signal periods, the signal light uses the timing scheme in the corresponding period. Otherwise, the signal timing scheme conflicts in the same signal period. Because the intersection cannot implement 2 timing schemes in the same signal period.

Handle conflicts and repair infeasible solutions. A simple rule for handling conflicting requests is the FIFS policy. However, it has been discovered that the FIFS is not an excellent solution to handle conflicts (Ye, Xu 2017). Another way to handle conflicts is to set priorities for different TSP schemes. Priority represents the necessity for a single bus to need priority signals, which is determined by the current operating conditions (Kim *et al.* 2012), such as headway delay, the number of passengers on board, bus delay, and so on. In this scheme, headway delay is selected as the index to evaluate requests. The headway delay is expressed as:

$$t_{hdd} = T_{i-n}^k - T_{i-(n-1)}^k - \Delta t_d, \quad (14)$$

where: t_{hdd} is the headway delay; T_{i-n}^k is the arriving time at S_k for the nth bus in the ith bus line.

Comparing the head delay between each bus and its adjacent front buses in the same line, the coding of buses with larger headway delay is used (i.e., execute the signal timing requirements of buses with larger headway delay). The larger headway delay means that the distance between 2 adjacent buses is far, which may lead to the long waiting time for passengers on this route. Therefore, the signal timing scheme of this route is given priority. Although headway delay is used to handle the conflict of signal timing scheme, it does not contradict the optimization goal of minimizing passengers waiting time. Headway delay is only a judgment index for the solution of the signal conflict, which has little impact on the joint optimization results of the whole line.

Discussion on buses passing through intersections. The joint optimization strategy improves the priority of buses passing through intersections. There are several possible situations for the control results of the joint optimization scheme:

- as shown in Figure 8a, buses need to stop and wait at the intersection before optimization. By using the joint optimization of speed guidance and signal control, the bus could directly pass through the intersection;

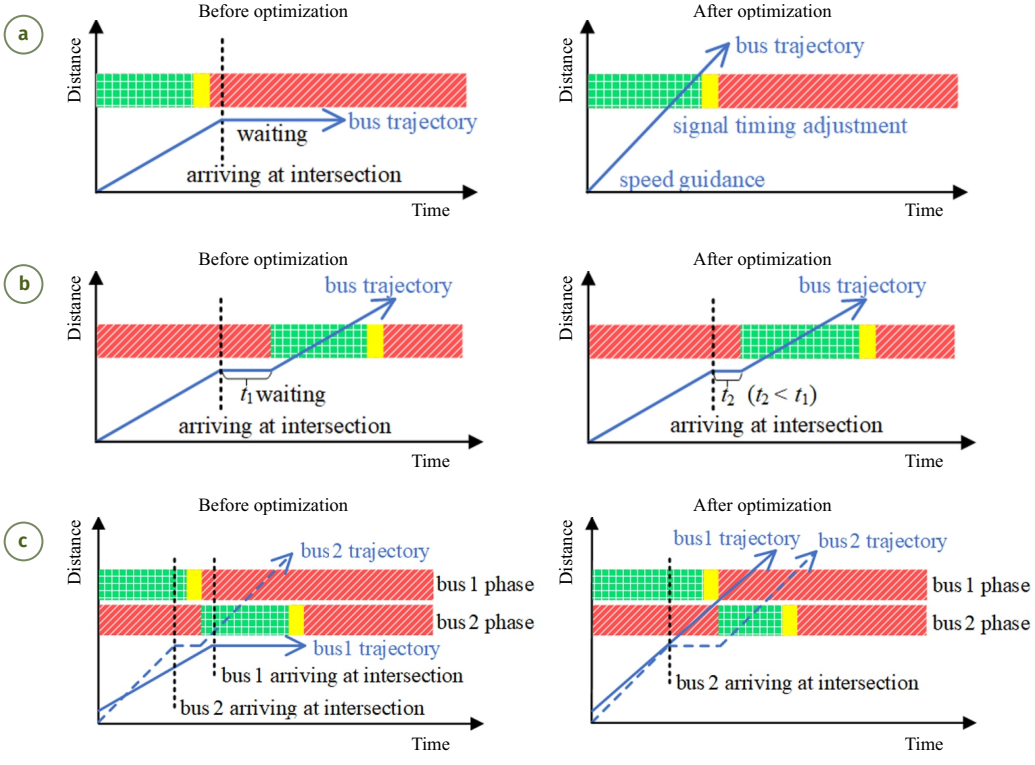

Figure 8. Sample situations of buses passing through an intersection:
(a) – a bus passing directly through the intersection; (b) – a bus cannot pass through the intersection;
(c) – multiple buses passing through the intersection

- as shown in Figure 8b, buses may have to wait at the intersection in some scenarios. Although the joint optimization scheme is used, the bus still cannot pass through the intersection directly. The reason is that the constraints of speed and signal light affect the optimization results. For example, speed cannot be guided on non-DBLs, and the single signal control cannot achieve satisfactory results. Moreover, due to various uncertain factors in real-world driving, such as traffic accidents and human factors, the implementation effect of the joint optimization strategy is impacted. This also leads to the parking and waiting of some buses;
- as shown in Figure 8c, when multiple buses pass through one intersection in the same signal period, the timing scheme of the bus with the larger headway delay is executed for the conflict of signals. Therefore, other buses at this intersection need to wait.

Although the above scenarios exist, the optimization interval is short. Thus, the influence of uncertain factors is small in one optimization interval and could be handled in time in the next optimization interval. Generally, the scheme is to improve the priority of buses.

Non-priority phase compensation. The joint optimization strategy improves the priority of buses at intersections, which may affect non-priority vehicles. For example, when the bus passes through the intersection by extending the green light of the priority phase, the green lights of the non-priority phases are shortened. The reason is that one signal period C_{light} is fixed. Therefore, after the bus passes through the intersection, compensating for the non-priority signal phase is beneficial to enhance the traffic capacity in the non-priority direction (Lian *et al.* 2020). The signal priority strategy only adjusts the signal timing in the corresponding bus-passing period. When no bus passes through the intersection, the phase-time loss in other non-priority directions could be compensated:

- in Figure 9a, to improve bus priority with east-west through to pass through intersections, the duration of non-priority phases 1&5 is reduced by t_e in the previous bus passing period;
- in Figure 9b, the duration of non-priority phases 1&5 is compensated by t_e in the next signal period without bus passing. The signal priority is constrained by Equation (12). Thus, the compensation signal is also constrained. This is good to reduce the impact on social vehicle travel time and decrease the probability of traffic congestion.

4.3. TSSA

In this study, the model formulation takes into account the real bus operation scenario involving multiple lines, various constraints, and complex nonlinear factors, which cannot be solved by conventional mathematical programming methods. Therefore, a meta-heuristic algorithm named TSSA is designed to compute the approximate optimal solution.

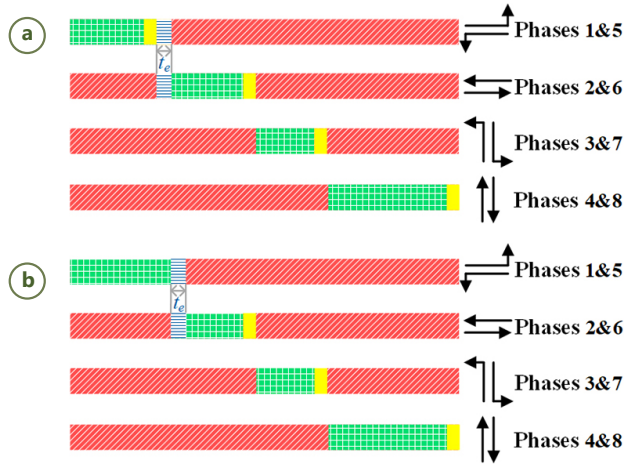

Figure 9. The example of intersection signal control and compensation:
(a) – the duration of non-priority phases 1&5 is affected;
(b) – the duration of non-priority phases 1&5 is compensated

Specifically, SSA is a swarm intelligence optimization algorithm in a meta-heuristic algorithm proposed by Mirjalili *et al.* (2017). SSA simulates the group behaviour of salps when they move and forage in the ocean, and is a novel algorithm for solving single-objective optimization problems. SSA has the advantages of simple structure, few parameters, and easy operation. However, similar to other swarm intelligence algorithms, SSA also suffers from slow convergence speed, loss of population diversity in the late iteration, and difficulty in balancing its exploration and exploitation. Therefore, SSA can be improved to address these issues by introducing asexual and sexual reproduction (Section 4.3.2) and multi-pattern search foraging (Section 4.3.3) in TSSA.

Moreover, compared with the exact algorithm, the meta-heuristic algorithm can obtain satisfactory solutions in the limited time for large-scale problems, which is more suitable for online scheduling. In MATLAB (*https://se.mathworks.com*), the computation time of running TSSA once is about 27.96 s when the number of iterations is 400 and population size is 50. This computation time is much less than the optimization interval (i.e., 150 s). This means that TSSA could satisfy the real-time requirement as an online algorithm.

Note that a salp of TSSA is the real-coding sequence corresponding to a solution of adjusting bus speed on DBLs V_{i-n}^{m} and intersection signal timing p_u. And the best solution (i.e., the best fitness salp) of TSSA is the output of TSSA, which is the decision variable.

4.3.1. Algorithm procedure

As a new variant of the SSA (Mirjalili *et al.* 2017), TSSA is inspired by the salp philosophies of asexual and sexual reproduction and multi-pattern search foraging. The procedure of TSSA is shown in Figure 10, and its pseudocode is given in Algorithm 1. TSSA simulates the asexual

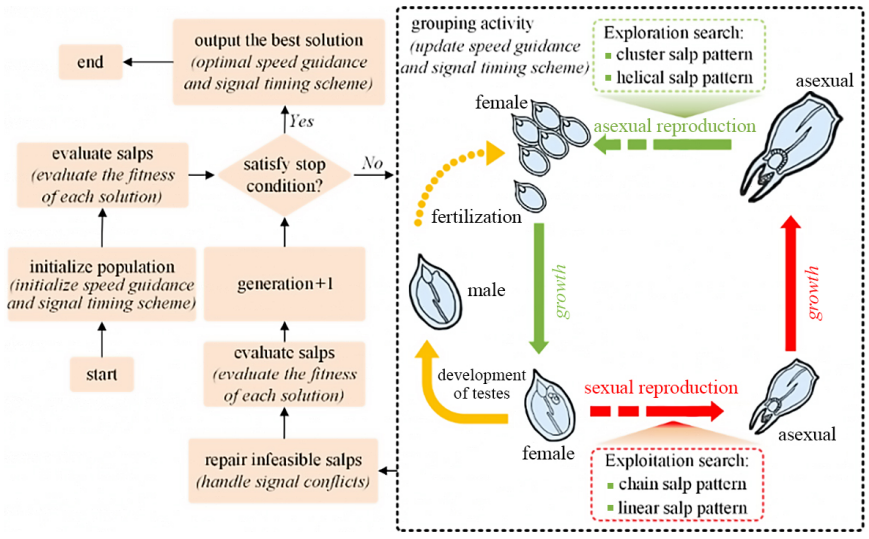

Figure 10. The procedure of TSSA

and sexual reproduction mechanisms of salp swarms to balance exploitation search effort and exploration search effort. Furthermore, TSSA simulates the foraging behaviours of 4 patterns (i.e., chain salp, linear salp, cluster salp, and helical salp patterns) to ensure the search-behaviour diversity of salp swarms.

4.3.2. Asexual and sexual reproduction

TSSA simulates the grouping activity of the population to achieve the coexistence of multiple salp patterns. The grouping activity strategy is the important kernel of TSSA. Salps are divided into 2 groups according to fitness. The 1st 50% of individuals are updated by chain salp pattern search or linear salp pattern search. The 2nd 50% are updated by cluster salp pattern search or helical salp pattern search. In the iterative process, exploitation and exploration always coexist to realize multi-pattern search behaviours.

As shown in Figure 10, salp reproduction ways are constantly changing due to environmental influences:

- ***sexual reproduction***: in the bad times when food is scarce, salps create multiple candidate genes through sexual reproduction. This reproduction mechanism could retain favourable genotypes and eliminate unfavourable ones to ensure population quality;
- ***asexual reproduction***: in the favourable conditions of abundant food, salps amplify the favourable genotypes through asexual reproduction, resulting in exponential population growth.

Algorithms 2 and 3 introduce sexual reproduction and asexual reproduction. Generally, salp warms alternate between asexual and sexual reproduction. This special life cycle enables salps to have high fertility, low generation time, and high survival rate.

Algorithm 1: *TSSA*	
1	initialize the salp population X^i, i = 1, 2, ..., N_{ps}
2	evaluate each salp X^i
3	while (stop condition is not satisfied)
4	rank salps according to fitness
5	F^*= the best solution X^* (the best fitness salp)
6	update the leader salp X^1 by using the 2nd-best fitness salp
7	grouping activity
8	amend the salps based on the upper and lower bounds and repair infeasible salps
9	evaluate each salp X^i
10	end
11	return X^*

Algorithm 2: *Sexual reproduction*	
1	evaluate the front 50% updated population
2	rank salps according to fitness
3	randomly generate the number of eliminating the poor fitness salps N_e; N_e should satisfy the low limit constraint of population size (i.e., population size ≥ the low limit of population size)
4	according to N_e, delete the poor fitness salps from the front 50% updated population

Algorithm 3: *Asexual reproduction*	
1	randomly generate the number of the new-born salps N_p; N_p should satisfy the upper limit constraint of population size (i.e., population size ≤ the upper limit of population size)
2	randomly select N_p salps from the back 50% updated population
3	for each selected slap, select a coding segment, use random mutation, and obtain new-born salps
4	copy these new-born salps into the back 50% updated population

4.3.3. Multi-pattern search foraging

Through the long history of evolution, salps form a unique way of swimming and foraging. There is a variety of arrangement patterns in Figure 11 (Madin 1990).

Two patterns of exploitation search. Exploitation search (i.e., intensification search) is defined as the swimming that salps move towards the food source F^*. The chain and linear salps both have leader, followers, and F^*, which are determined: according to fitness, the best fitness salp in the population is defined as F^*. Then, in the chain salp swarm (or linear salp swarm), the best fitness salp is defined as the leader, and other salps are followers:

1) ***The chain salp pattern search.*** In Figure 11a, chain salps are at right angles to the chain axis. In the salp chain, the leader salp at the front is to guide the salp chain by using:

$$x_j^1 = \begin{cases} a_1, & 0.5 \le c_1 \le 1; \\ a_2, & 0 \le c_1 < 0.5; \end{cases} \tag{15}$$

$$a_1 = f_j + 2 \cdot e^{-\left(\frac{4 \cdot l}{L}\right)^2} \cdot \left(\left(ub_j - lb_j\right) \cdot c_2 + lb_j\right);$$

$$a_2 = f_j - 2 \cdot e^{-\left(\frac{4 \cdot l}{L}\right)^2} \cdot \left(\left(ub_j - lb_j\right) \cdot c_2 + lb_j\right),$$

where: x_j^1 is the jth position of the leader X^1; f_j is the jth position of the food source F^* (i.e., the best solution X^*); ub_j ub_j, lb_j are the upper and lower bound of the jth position, respectively; $c_1 \in [0,1]$, $c_2 \in [0,1]$, and they are random numbers; c_1 indicates if the next position in jth position should be towards positive infinity or negative infinity; c_2 indicates a random number between 0 and 1; l is the current generation number; L is the maximum number of iterations.

The position of the follower is updated by:

$$x_j^i = \frac{1}{2} \cdot \left(x_j^i + x_j^{i-1}\right), \tag{16}$$

where: x_j^i is the position of the ith follower in the jth position; $i \ge 2$;

2) ***The linear salp pattern search.*** In Figure 11b, linear salps are arranged along the axis of the chain and connected with opposite, anterior, and posterior animals. The leader L^1 is also updated by using Equation (15). For followers (i.e., other linear salps L^i and $i \ge 2$), the angle of linear salps with the chain axis is defined as φ. 1st, randomly select N_g consecutive genes. Then, randomly generate an angle from 0° to 90° as φ. The selected jth position of the ith salp is updated by:

$$l_j^i = l_j^{i-1} - \sin\varphi \cdot \left(l_j^{i-1} - l_j^i\right), \tag{17}$$

where: l_j^i is the jth position of the ith salp.

In principle, Equation (17) ensures that each linear salp moves closer to the previous follower.

Two patterns of exploration search. Exploration search (i.e., diversification search) is defined as the swimming that salps move away from the food source F^*:

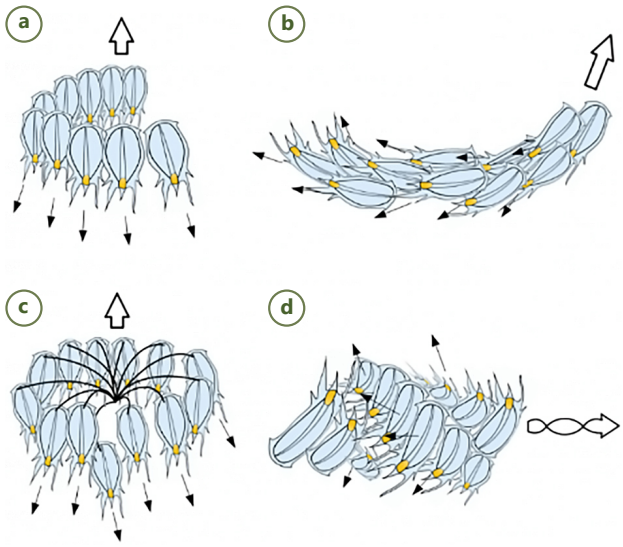

Figure 11. Patterns of arrangement of aggregate salps:
(a) – chain salp pattern;
(b) – linear salp pattern;
(c) – cluster salp pattern;
(d) – helical salp pattern

1) ***The cluster salp pattern search.*** In Figure 11c, each slap in cluster salps is connected by a long ventral peduncle to the cluster's center. The shape of clusters is irregular. The cluster center is defined as F^* (i.e., salp with the best fitness). These cluster salps always move away from F^*. In the cluster salps, the jth position of the ith salp c_j^i is updated by:

$$c_j^i = \begin{cases} b_1, & f_j - c_j^i \le 0; \\ b_2, & f_j - c_j^i > 0; \end{cases} \tag{18}$$

$$b_1 = c_j^i + a \cdot e^{-\frac{l}{L}} \cdot \frac{1}{3}\left(ub_j - lb_j\right);$$

$$b_2 = c_j^i - a \cdot e^{-\frac{l}{L}} \cdot \frac{1}{3}\left(ub_j - lb_j\right),$$

where: l is the current generation number; L is maximum number of iterations; a is a random number from 0 to 1; f_j is the jth position of F^*; $\left(ub_j - lb_j\right)/3$ limits the variation of c_j^i to fit the coding range; $e^{-\frac{l}{L}}$ controls the outward exploration of cluster slaps.

With l increasing, $e^{-\frac{l}{L}}$ gradually decreases the outward expansion of the distance between the slap and F^*;

2) ***The helical salp pattern search.*** In Figure 11d, the highly asymmetric salps explore forward in the form of a dual helix. In the helical salps, the jth position of the ith salp h_j^i is updated by:

$$h_j^i = \begin{cases} c_1, & f_j - h_j^i \le 0; \\ c_2, & f_j - h_j^i > 0; \end{cases} \tag{19}$$

$$c_1 = h_j^i + \frac{1}{2} \cdot D \cdot e^{-\left(\frac{l}{L}\right)^2} \cdot \left(\cos\left(5 \cdot 2 \cdot \pi \cdot a \cdot \frac{l}{L}\right) + 1\right);$$

$$c_2 = h_j^i - \frac{1}{2}\cdot D\cdot e^{-\left(\frac{l}{L}\right)^2}\cdot\left(\sin\left(5\cdot 2\cdot\pi\cdot a\cdot\frac{l}{L}\right)+1\right),$$

where: $D = \left|f_j - h_j^i\right|$; $|\cdot|$ is the absolute value; f_j is the jth position of F^*; a is a random number from 0 to 1; $e^{-\left(\frac{l}{L}\right)^2}$ controls the outward exploration of helical slaps.

Generally, with generation increasing, many combinations of chain salp, linear salp, cluster salp, and helical salp patterns are generated by using the grouping activity. This is the cornerstone of steadily improving TSSA's search performance. On the other hand, cluster salp and helical salp patterns are based on the circle and helical curve equations. Equations (18) and (19) are usually used for exploitation search (i.e., intensification search). In previous studies, the circle and helical curve equations are rarely applied to exploration search (i.e., diversification search).

5. Case study

5.1. Description of network and data

On test problems. The bus data in Beijing Bus Group are used to construct 6 test problems in Table 1. These data include the actual operation information of multi-bus-lines, bus stops, intersections, distances, DBL, non-DBLs, and so on. This is consistent with the real road networks, as shown in Figure 12.

On experimental metrics. Referring to (Chen *et al.* 2015), passenger demand ρ is defined as a passenger flow multiplicator. Passenger demand ρ = 1 means that the time-varying passenger flow is daily passenger flow (see Figure 4). Passenger demand ρ = 2 implies that the time-varying passenger flow is 2 × daily passenger flow. Moreover, the AWTP $\bar{w}$ in Equation (20) and the AHDR $\bar{r}_{hd}$ in Equation (21) are used as evaluation criteria. Note that the AWTP calculation includes all bus stops of all bus lines in one day.

$$\bar{w} = \frac{\sum_{i=1}^{N_l}\sum_{k=1}^{N_{si}-1}\sum_{n=1}^{N_{bi}} w_{i-n}^k}{\sum_{i=1}^{N_l}\sum_{k=1}^{N_{si}-1}\int_{D_{i-1}}^{T_{i-N_{bi}}^k}\lambda_i^k(t)\,\mathrm{d}t}; \tag{20}$$

$$\bar{r}_{hd} = \frac{\sum_{i=1}^{N_l}\sum_{k=1}^{N_{si}}\sum_{n=2}^{N_{bi}}\left(T_{i-n}^k - T_{i-(n-1)}^k\right)}{\sum_{i=1}^{N_l}\left(N_{si}\cdot\left(N_{bi}-1\right)\right)} - \Delta t_d}{\Delta t_d}\cdot 100\%, \tag{21}$$

where: Δt_d is the departure interval, Δt_d = 15 min.

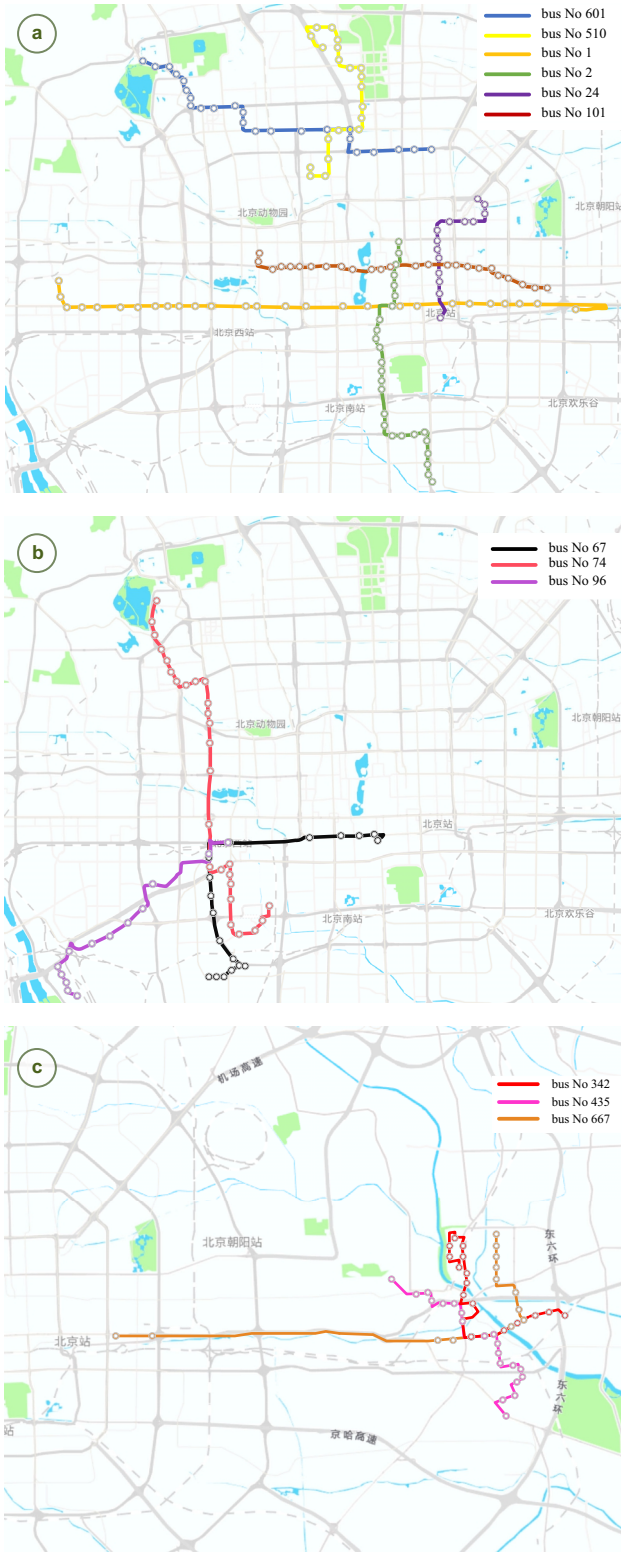

Figure 12. Multi-bus-lines of the real road networks in Beijing:
(a) – test problems F1...F4;
(b) – test problem F5;
(c) – test problem F6

On comparison data. The sources of comparison data are divided into 2 groups as follows:

- the 1st group is used to demonstrate the effectiveness of the multi-bus-line joint operation strategy. The actual operation data from Beijing Bus Group is used to represent the non-optimized result without speed guidance and signal priority. The non-optimized result comes from the statistical bus traveling data on 15 August 2021, in Beijing;
- the 2nd group is used to demonstrate the general performance of TSSA, including MBGA (Luo *et al.* 2019), SSA (Mirjalili *et al.* 2017), and SHC (Gkiotsalitis 2021) as compared algorithms (i.e., replacing TSSA with one compared online optimization algorithm, as shown in Figure 5). These algorithms use the same population initialization and repair strategy as TSSA. Moreover, they use the same decision variables as TSSA to jointly optimize signal priority and speed control. SHC and MBGA use the rescheduling strategy based on a rolling horizon idea. MBGA stores the information of high-quality historical solutions into the memory for updating the next generation population. SHC considers the bus layover and capacity constraints and obtains a near real-time rescheduling solution by exploring only part of the whole-day timetable. In addition, exact algorithms are not selected for comparison because they usually cannot meet the requirement of online optimization intervals.

Table 2 provides the used parameter setting in this article.

Note that, the boarding time of passengers is easy to obtain from bus billing systems in practice. However, the time of passengers arriving at stops is challenging to monitor and obtain. Thus, obtaining real data of passengers waiting time is not very easy. Therefore, the simulation data of passengers waiting time is used based on some real historical data of passenger flow in Figure 4. The total number of passengers in these test problems is large, such as 17206 passengers in F1 and 37466 passengers in F6.

Table 1. Test problems

Problem	N_l	N_i	N_s	N_r	Bus lines	Total number of passengers
F1	1	10	24	33	601	17206
F2	1	18	25	42	510	15891
F3	2	29	45	83	1, 2	27027
F4	2	26	39	64	24, 101	30288
F5	3	15	56	71	67, 74, 96	34513
F6	3	24	53	76	342, 435, 667	37466

Notes: N_l is the number of bus lines; N_i is the number of intersections; N_s is the number of stops; N_r is the number of roads.

5.2. Comparison of the AWTP

Passenger satisfaction is important to make more passengers travel by buses instead of private vehicles. And AWTP is a critical factor in evaluating passenger satisfaction. Smaller AWTP, better passenger satisfaction. In this section, only TSSA is compared with the 3 compared online optimization algorithms and not with the actual data of passengers waiting time. The reason is that real data of passengers waiting time cannot be obtained. There are 2 kinds of comparisons:

- daily passenger flow;
- different level passenger flow.

On AWTP for daily passenger flow. Figure 13 presents the mean of AWTP results for daily passenger flow. TSSA is better than other algorithms in all cases. For example, for all 17206 passengers in the F1 test problem, the AWTP difference between MBGA and TSSA is 5850.04 min (i.e., $17206 \cdot (7.79 - 7.45) = 5850.04$). Besides, with the test problem size increasing, TSSA could always obtain AWTP performance. Compared with SSA, TSSA has an obvious performance improvement. Moreover, the standard deviation of TSSA is very small. This shows that it is no coincidence that TSSA obtains the optimal solution, but always maintains stable performance. The reason is that TSSA makes full use of asexual and sexual reproduction and multi-pattern search foraging. This also indicates that the grouping activity of salp swarms could balance exploitation search effort and exploration search effort. In addition, premature convergence is also a common pain point of swarm intelligence optimization. TSSA introduces cluster salp and helical salp patterns, which use reverse diffusion to prevent premature convergence. The results show that many combinations of multi-pattern search are effective to ensure the search performance of TSSA.

On Wilcoxon results for AWTPs. To further demonstrate the effectiveness of TSSA, the Wilcoxon test is used with a significance level of 0.05 for AWTPs in 20 runs. In Table 3, the symbols of $(+)$, $(\approx)$, and $(-)$ indicate that TSSA is superior to, approximately equivalent to, and inferior to one compared algorithm, respectively. In all test problems, TSSA outperforms other compared algorithms.

Table 2. Used parameter setting

Items	Parameters
SHC	population size N_{ps} = 50
MBGA	population size N_{ps} = 50; the crossover rate P_c = 0.85; the mutation rate P_m = 0.1
TSSA	population size N_{ps} = 50; the upper limit of population size = 54; the low limit of population size = 12
SSA	population size N_{ps} = 50
Stop condition	stop condition is that the number of using the fitness functions = 20000; for example, by using SHC, its maximum generation is 400 (i.e., 20000/50 = 400).

On AWTP for different level passenger flow. The increase of passenger flow usually leads to a significant increase in the waiting time of passengers. This is an important reason why passengers are unwilling to travel by bus. Therefore, to demonstrate the passenger satisfaction performance for different level passenger flows, Figure 14 presents the mean of AWTPs when passenger demand ρ = 0.2, 0.6, 1.4, 1.8. In Figure 14, TSSA outperforms others in all cases. Moreover, TSSA has more obvious advantages in Figure 14 than in Figure 13, especially for the high-level passenger flow (like passenger demand ρ = 1.8). This also means that the multi-bus-line joint operation strategy could ensure passenger satisfaction, even for high-level passenger flows.

Generally, these results indicate that the multi-bus-line joint operation strategy is effective to minimize passengers waiting time. Moreover, TSSA could provide better results of the waiting time for daily passenger flow and different level passenger flow.

Table 3. Wilcoxon results for AWTPs in 20 runs between one compared algorithm and TSSA when using daily passenger flow (i.e., passenger demand ρ = 1.0)

Algorithm	Problem						*Sum* (+)	*Sum* (–)
	F1	F2	F3	F4	F5	F6		
SHC	+	+	+	+	+	+	6	0
SSA	+	+	+	+	+	+	6	0
MBGA	+	+	+	+	+	+	6	0

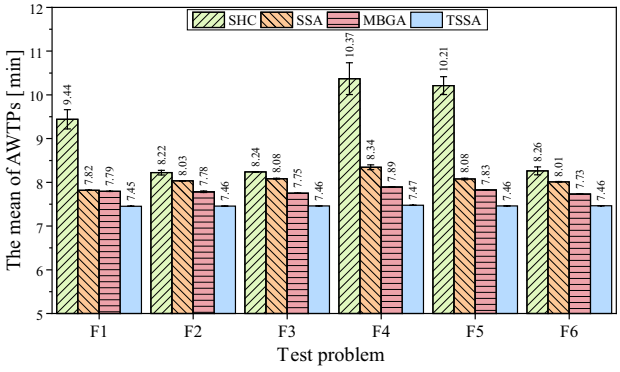

Figure 13. The mean of AWTPs for 20 runs when using daily passenger flow (i.e., passenger demand ρ = 1.0)

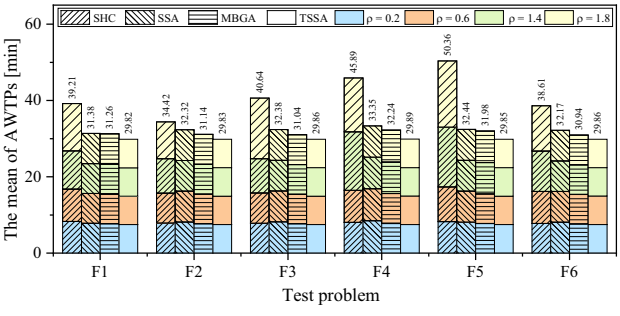

Figure 14. The mean of AWTPs for 20 runs when using different level passenger flows (i.e., passenger demand ρ = 0.2, 0.6, 1.4, 1.8)

5.3. Comparison of the AHDR

On AHDR. AHDR is one of the most important factors to evaluate the stability of bus service. Smaller AHDR, better stability of the bus service. To explore the feasibility of TSSA in practical application, TSSA is compared with the non-optimized result and 3 compared algorithms. The non-optimized result comes from the statistical bus traveling data on 15 August 2021, in Beijing. Figure 15 presents the AHDR results for all test problems. In all cases, all algorithms are better than the non-optimized result (i.e., results without speed guidance and signal priority). This implies that the multi-bus-line joint operation strategy is effective to ensure the better stability of bus service. Meanwhile, the AHDR results of TSSA are the 1st-best or 2nd-best. This demonstrates that TSSA could also ensure the AHDR performance.

On the headway deviation ratio for daily passenger flow. Morning rush hours are the key point for evaluating the stability of bus service. To observe the morning-rush-hour situation for daily passenger flow, Figure 16 shows the bus headway deviation ratio at each stop of 10 buses departing from 8:00 AM and 10:30 AM for F1. The headway deviation ratio of 2 adjacent buses is greatly affected by headway. For example, one bus arrives at the stop S_k at 8:30 AM, and the next bus arrives at S_k at 8:48 AM. The headway between them is 18 min, and the departure interval is 15 min. Thus, the headway deviation ratio is 20% (i.e., $|18-15|/15\cdot100\%$). The headway is affected by traffic and passengers. Besides, the stop behind accumulates the impact of all previous stops. Thus, the headway between adjacent buses is unstable, which leads to great fluctuations in the headway deviation ratio curve.

The stability of bus service is evaluated from the fluctuation and numerical value of the headway deviation ratio curve. From a curve-fluctuation perspective, comparing Figure 16a with Figures 16b~16e, the headway deviation ratio of each algorithm is more stable than the non-optimized result. Besides, the curve fluctuation results of TSSA are the 2nd-best. Moreover, from a numerical perspective, TSSA's results are also the 2nd-best. Generally, the AHDR results of TSSA are satisfactory in most parts of the morning-rush-hour.

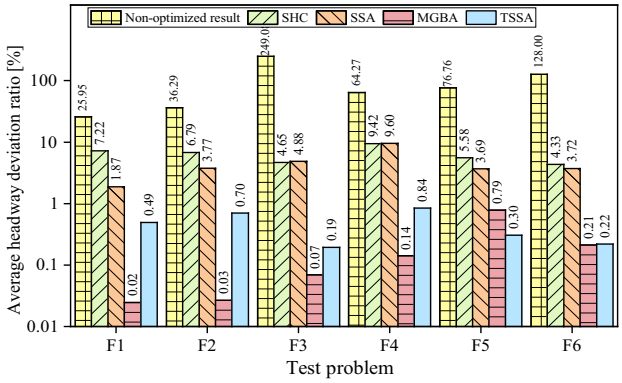

Figure 15. The AHDR for all test problems when using daily passenger flow (i.e., passenger demand ρ = 1.0)

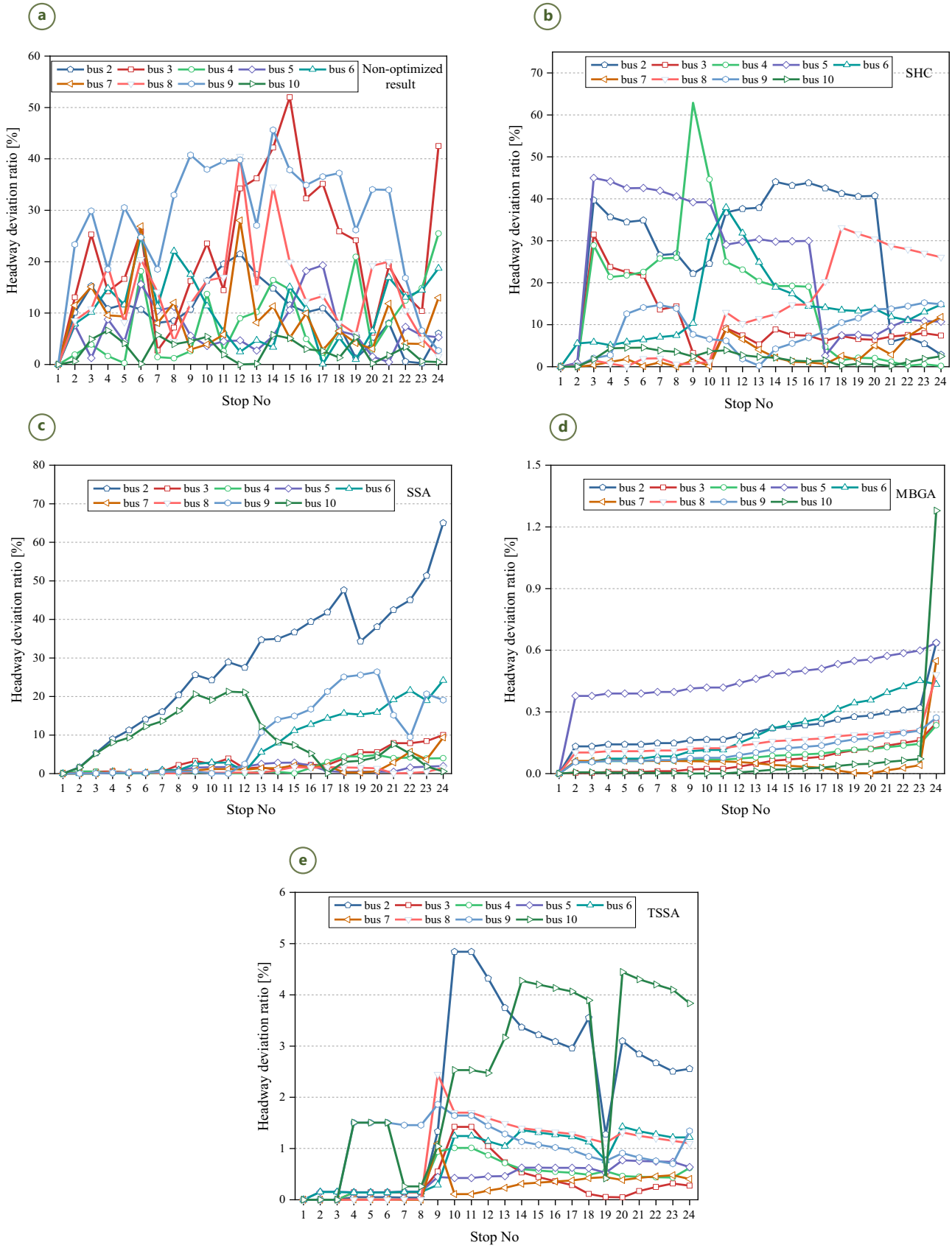

Figure 16. Bus headway deviation ratio at different stops between 8:00 AM and 10:30 AM for test problem F1 when using daily passenger flow (i.e., passenger demand ρ = 1.0):

(a) – non-optimized result; (b) – SHC; (c) – SSA; (d) – MBGA; (e) – TSSA

On the headway deviation ratio for high-level passenger flow. To further demonstrate the AHDR performance for high-level passenger flow (i.e., passenger demand ρ = 2.0), Figure 17 presents the headway deviation ratio of each stop of 10 buses departing from 8:00 AM and 10:30 AM for F1. The actual data for high-level passenger flow cannot be obtained. Therefore, only TSSA is compared with 3 optimization algorithms. Similar to Figure 16, the curves in Figure 17 are still fluctuating. Besides, since the passenger demand doubles and the passenger boarding and alighting time doubles, the headway deviation ratio in Figure 17 is worse than that in Figure 16.

Compared with Figure 16, these headway deviation results of each algorithm get worse. However, from the perspective of numerical increase, the headway-deviation increase of TSSA is relatively small (i.e., the maximum value increases from 5 to 8). Moreover, from a curve-trend perspective, the curve-fluctuation results of TSSA are still the 2nd-best. Generally, these results indicate that the joint operation strategy could optimize the waiting time of passengers and provide satisfactory headway performance.

6. Conclusions

For the real requirements of intelligent bus systems in Beijing, the real-time framework of the multi-bus-line joint operation strategy is designed. The goal is to minimize the passengers waiting time of multi-bus-lines to improve the efficiency of ground transportation networks. In this work, the practicality and effectiveness of the proposed joint operation strategy are highlighted. From the perspective of practicality, the intelligent bus system model fully considers many practical factors, such as real road conditions and bus operation situations. From the perspective of

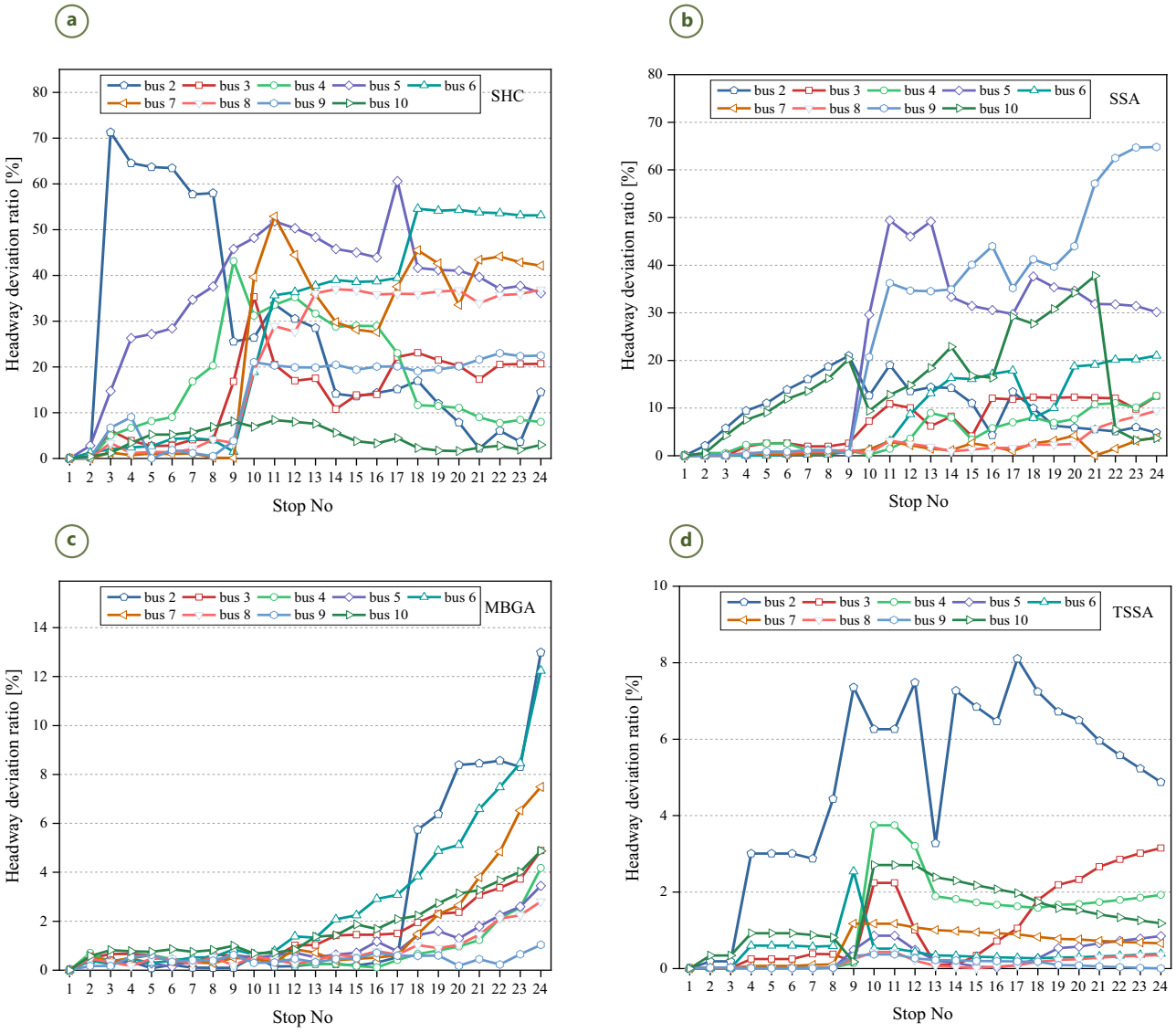

Figure 17. Bus headway deviation ratio at different stops between 8:00 AM and 10:30 AM for test problem F1 when using high-level passenger flow (i.e., passenger demand ρ = 2.0):
(a) – SHC; (b) – SSA; (c) – MBGA; (d) – TSSA

effectiveness, the multi-bus-line joint operation strategy is designed, which considers signal conflict and non-priority phase delay. Then, TSSA is developed as an online optimization algorithm, and the effectiveness of this method is evaluated. As a result, it can be stated that this strategy can indeed improve the availability and stability of bus system services. However, the proposed method does not consider the impact of time-varying traffic congestion on real-time speed change in different sections.

In the future, the research will focus on the impact of time-varying traffic flow on bus dispatching. Besides, the application of artificial intelligence algorithms in transportation will also be further explored. For example, with the rapid development of parallel computing, designing a parallel algorithm with fast operation speed and suitable for large-scale DVRP is worthy of further study. Moreover, based on emerging technologies such as big data, cloud computing, and the Internet of Things, the traffic management center will gather information from people, vehicles, roads, stations, environments, and other public transport elements to conduct diversified integration, analysis, and processing of various dynamic data.

Acknowledgements

The authors would like to thank for supporting this research:

- National Natural Science Foundation of China (Grants No 62376036, 61876199);
- Research Initiative of Ideological and Political Theory Teachers (Grant No 20SZK10013001).

Funding

The authors disclosed receipt of the following financial support for the research, authorship, and/or publication of this article.

This work was supported by:

- National Natural Science Foundation of China (Grants No 62376036, 61876199);
- Research Initiative of Ideological and Political Theory Teachers (Grant No 20SZK10013001).

Disclosure statement

The authors declared no potential conflicts of interest with respect to the research, authorship, and/or publication of this article.

Author contributions

Hong Guang Zhang was conceived the study and was responsible for the design and development of the data analysis.

Ting Ting Liu and *Xiang Li* were responsible for data collection and investigation.

Yuan An Liu and *Xiang Li* were responsible for visualization.

Hong Guang Zhang and *Ting Ting Liu* wrote the original draft.

Hong Guang Zhang was responsible for the writing, review and editing, so the final article.

All authors read and agreed to the published version of the manuscript.

References

Ampountolas, K.; Kring, M. 2021. Mitigating bunching with bus-following models and bus-to-bus cooperation, *IEEE Transactions on Intelligent Transportation Systems* 22(5): 2637–2646. https://doi.org/10.1109/tits.2020.2973585

Anderson, P.; Daganzo, C. F. 2020. Effect of transit signal priority on bus service reliability, *Transportation Research Part B*: *Methodological* 132: 2–14. https://doi.org/10.1016/j.trb.2019.01.016

Asgharzadeh, M.; Shafahi, Y. 2017. Real-time bus-holding control strategy to reduce passenger waiting time, *Transportation Research Record*: *Journal of the Transportation Research Board* 2647: 9–16. https://doi.org/10.3141/2647-02

Bian, B.; Zhu, N.; Pinedo, M.; Ma, S.; Yu, Q. 2020. An optimization-based speed-control method for high frequency buses serving curbside stops, *Transportation Research Part C*: *Emerging Technologies* 121: 102860. https://doi.org/10.1016/j.trc.2020.102860

Chen, J.; Liu, Z.; Zhu, S.; Wang, W. 2015. Design of limited-stop bus service with capacity constraint and stochastic travel time, *Transportation Research Part E*: *Logistics and Transportation Review* 83: 1–15. https://doi.org/10.1016/j.tre.2015.08.007

Colombaroni, C.; Fusco, G.; Isaenko, N. 2020. A simulation-optimization method for signal synchronization with bus priority and driver speed advisory to connected vehicles, *Transportation Research Procedia* 45: 890–897. https://doi.org/10.1016/j.trpro.2020.02.079

Dadashzadeh, N.; Ergun, M. 2019. An integrated variable speed limit and ALINEA ramp metering model in the presence of high bus volume, *Sustainability* 11(22): 6326. https://doi.org/10.3390/su11226326

Daganzo, C. F.; Pilachowski, J. 2011. Reducing bunching with bus-to-bus cooperation, *Transportation Research Part B*: *Methodological* 45(1): 267–277. https://doi.org/10.1016/j.trb.2010.06.005

Deng, Y.-J.; Liu, X.-H.; Hu, X.; Zhang, M. 2020. Reduce bus bunching with a real-time speed control algorithm considering heterogeneous roadway conditions and intersection delays, *Journal of Transportation Engineering*, *Part A*: *Systems* 146(7): 04020048. https://doi.org/10.1061/jtepbS.0000358

Ghanim, M. S.; Abu-Lebdeh, G. 2015. Real-time dynamic transit signal priority optimization for coordinated traffic networks using genetic algorithms and artificial neural networks, *Journal of Intelligent Transportation Systems*: *Technology*, *Planning*, *and Operations* 19(4): 327–338. https://doi.org/10.1080/15472450.2014.936292

Gkiotsalitis, K. 2021. Bus rescheduling in rolling horizons for regularity-based services, *Journal of Intelligent Transportation Systems*: *Technology*, *Planning*, *and Operations* 25(4): 356–375. https://doi.org/10.1080/15472450.2019.1681992

Gkiotsalitis, K.; Wu, Z.; Cats, O. 2019. A cost-minimization model for bus fleet allocation featuring the tactical generation of short-turning and interlining options, *Transportation Research Part C*: *Emerging Technologies* 98: 14–36. https://doi.org/10.1016/j.trc.2018.11.007

Gong, S.; Zhou, A.; Peeta, S. 2019. Cooperative adaptive cruise control for a platoon of connected and autonomous vehicles considering dynamic information flow topology, *Transportation Research Record*: *Journal of the Transportation Research Board* 2673(10): 185–198. https://doi.org/10.1177/0361198119847473

Hao, B.-B.; Lv, B.; Chen, Q. 2021. A bus signal priority model at oversaturated intersection under stochastic demand, *Mathematical Problems in Engineering* 2021: 2741094. https://doi.org/10.1155/2021/2741094

He, S.-X.; Dong, J.; Liang, S.-D.; Yuan, P.-C. 2019. An approach to improve the operational stability of a bus line by adjusting bus speeds on the dedicated bus lanes, *Transportation Research Part C*: *Emerging Technologies* 107: 54–69. https://doi.org/10.1016/j.trc.2019.08.001

He, S.-X.; Liang, S.-D.; Dong, J.; Zhang, D.; He, J.-J.; Yuan, P.-C. 2020. A holding strategy to resist bus bunching with dynamic target headway, *Computers & Industrial Engineering* 140: 106237. https://doi.org/10.1016/j.cie.2019.106237

Hounsell, N. B.; Shrestha, B. P.; Wong, A. 2012. Data management and applications in a world-leading bus fleet, *Transportation Research Part C*: *Emerging Technologies* 22: 76–87. https://doi.org/10.1016/j.trc.2011.12.005

Jia, H.; Lin, Y.; Luo, Q.; Li, Y.; Miao, H. 2019. Multi-objective optimization of urban road intersection signal timing based on particle swarm optimization algorithm, *Advances in Mechanical Engineering* 11(4): 1–9. https://doi.org/10.1177/1687814019842498

Kaiwartya, O.; Abdullah, A. H.; Cao, Y.; Altameem, A.; Prasad, M.; Lin, C.-T.; Liu, X. 2016. Internet of vehicles: motivation, layered architecture, network model, challenges, and future aspects, *IEEE Access* 4: 5356–5373. https://doi.org/10.1109/access.2016.2603219

Kim, S.; Park, M.; Chon, K. S. 2012. Bus signal priority strategies for multi-directional bus routes, *KSCE Journal of Civil Engineering* 16(5): 855–861. https://doi.org/10.1007/s12205-012-1507-7

Koonce, P.; Rodegerdts, L.; Lee, K.; Quayle, S.; Beaird, S.; Braud, C.; Bonneson, J.; Tarnoff, P.; Urbanik, T. 2008. *Traffic Signal Timing Manual*. Report No FHWA-HOP-08-024. US Department of Transportation, Federal Highway Administration (FHWA), Washington, DC, US. 274 p. Available from Internet: https://ops.fhwa.dot.gov/publications/fhwahop08024/fhwa_hop_08_024.pdf

Lee, W.-H.; Wang, H.-C. 2022. A person-based adaptive traffic signal control method with cooperative transit signal priority, *Journal of Advanced Transportation* 2022: 2205292. https://doi.org/10.1155/2022/2205292

Li, M.; Yin, Y.; Zhang, W.-B.; Zhou, K.; Nakamura, H. 2011. Modeling and implementation of adaptive transit signal priority on actuated control systems, *Computer-Aided Civil and Infrastructure Engineering* 26(4): 270–284. https://doi.org/10.1111/j.1467-8667.2010.00677.x

Li, R.; Jin, P. J.; Ran, B. 2016. Biobjective optimization and evaluation for transit signal priority strategies at bus stop-to-stop segment, *Mathematical Problems in Engineering* 2016: 1054570. https://doi.org/10.1155/2016/1054570

Li, S.; Liu, R.; Yang, L.; Gao, Z. 2019. Robust dynamic bus controls considering delay disturbances and passenger demand uncertainty, *Transportation Research Part B*: *Methodological* 123: 88–109. https://doi.org/10.1016/j.trb.2019.03.019

Lian, P.; Wu, Y.; Li, Z.; Keel, J.; Guo, J.; Kang, Y. 2020. An improved transit signal priority strategy for real-world signal controllers that considers the number of bus arrivals, *Sustainability* 12(1): 287. https://doi.org/10.3390/su12010287

Luo, X.; Liu, Y.; Yu, Y.; Tang, J.; Li, W. 2019. Dynamic bus dispatching using multiple types of real-time information, *Transportmetrica B*: *Transport Dynamics* 7(1): 519–545. https://doi.org/10.1080/21680566.2018.1447408

Madin, L. P. 1990. Aspects of jet propulsion in salps, *Canadian Journal of Zoology* 68(4): 765–777. https://doi.org/10.1139/z90-111

Mazloumi, E.; Currie, G.; Rose, G. 2010. Using GPS data to gain insight into public transport travel time variability, *Journal of Transportation Engineering* 136(7): 623–631. https://doi.org/10.1061/(asce)te.1943-5436.0000126

Miller, J. 2008. Vehicle-to-vehicle-to-infrastructure (V2V2I) intelligent transportation system architecture, in *2008 IEEE Intelligent Vehicles Symposium*, 4–6 June 2008, Eindhoven, Netherlands, 715–720. https://doi.org/10.1109/ivs.2008.4621301

Mirjalili, S.; Gandomi, A. H.; Mirjalili, S. Z.; Saremi, S.; Faris, H.; Mirjalili, S. M. 2017. Salp swarm algorithm: a bio-inspired optimizer for engineering design problems, *Advances in Engineering Software* 114: 163–191. https://doi.org/10.1016/j.advengsoft.2017.07.002

Moreira-Matias, L.; Mendes-Moreira, J.; De Sousa, J. F.; Gama, J. 2015. Improving mass transit operations by using AVL-based systems: a survey, *IEEE Transactions on Intelligent Transportation Systems* 16(4): 1636–1653. https://doi.org/10.1109/tits.2014.2376772

Saw, V.-L.; Vismara, L.; Chew, L. Y. 2020. Intelligent buses in a loop service: emergence of no-boarding and holding strategies, *Complexity* 2020: 7274254. https://doi.org/10.1155/2020/7274254

Schrank, D.; Eisele, B.; Lomax, T. 2012. *TTI's 2012 Urban Mobility Report*. Texas A&M Transportation Institute, Texas A&M University System, TX, US. 129 p. Available from Internet: https://static.tti.tamu.edu/tti.tamu.edu/documents/umr/archive/mobility-report-2012-wappx.pdf

Shan, X.; Chen, X.; Jia, W.; Ye, J. 2019. Evaluating urban bus emission characteristics based on localized MOVES using sparse GPS data in Shanghai, China, *Sustainability* 11(10): 2936. https://doi.org/10.3390/su11102936

Shang, H.-Y.; Huang, H.-J.; Wu, W.-X. 2019. Bus timetabling considering passenger satisfaction: an empirical study in Beijing, *Computers & Industrial Engineering* 135: 1155–1166. https://doi.org/10.1016/j.cie.2019.01.057

Tian, S.; Li, X.; Liu, J.; Ma, H.; Yu, H. 2022. A short-turning strategy to alleviate bus bunching, *Journal of Ambient Intelligence and Humanized Computing* 13(1): 117–128. https://doi.org/10.1007/s12652-020-02891-2

Varga, B.; Tettamanti, T.; Kulcsár, B. 2018. Optimally combined headway and timetable reliable public transport system, *Transportation Research Part C*: *Emerging Technologies* 92: 1–26. https://doi.org/10.1016/j.trc.2018.04.016

Wu, M.; Yu, C.; Ma, W.; An, K.; Zhong, Z. 2022. Joint optimization of timetabling, vehicle scheduling, and ride-matching in a flexible multi-type shuttle bus system, *Transportation Research Part C*: *Emerging Technologies* 139: 103657. https://doi.org/10.1016/j.trc.2022.103657

Wu, W.; Liu, R.; Jin, W. 2017. Modelling bus bunching and holding control with vehicle overtaking and distributed passenger boarding behaviour, *Transportation Research Part B*: *Methodological* 104: 175–197. https://doi.org/10.1016/j.trb.2017.06.019

Wu, W.; Ma, W.; Long, K.; Zhou, H.; Zhang, Y. 2016. Designing sustainable public transportation: integrated optimization of bus speed and holding time in a connected vehicle environment, *Sustainability* 8(11): 1170. https://doi.org/10.3390/su8111170

Xu, B.; Ban, X. J.; Bian, Y.; Li, W.; Wang, J.; Li, S. E.; Li, K. 2019. Cooperative method of traffic signal optimization and speed control of connected vehicles at isolated intersections, *IEEE Transactions on Intelligent Transportation Systems* 20(4): 1390–1403. https://doi.org/10.1109/tits.2018.2849029

Yang, K.; Menendez, M.; Guler, S. I. 2019. Implementing transit signal priority in a connected vehicle environment with and without bus stops, *Transportmetrica B*: *Transport Dynamics* 7(1): 423–445. https://doi.org/10.1080/21680566.2018.1434019

Ye, Z.; Xu, M. 2017. Decision model for resolving conflicting transit signal priority requests, *IEEE Transactions on Intelligent Transportation Systems* 18(1): 59–68. https://doi.org/10.1109/tits.2016.2556000

Zhang, Yi.; Su, R.; Zhang, Yic.; Wang, B. 2022. Dynamic multi-bus dispatching strategy with boarding and holding control for passenger delay alleviation and schedule reliability: a combined dispatching-operation system, *IEEE Transactions on Intelligent Transportation Systems* 23(8): 12846–12860. https://doi.org/10.1109/tits.2021.3117937

Zhao, H.; Feng, S.; Ci, Y. 2021. Scheduling a bus fleet for evacuation planning using stop-skipping method, *Transportation Research Record*: *Journal of the Transportation Research Board* 2675(11): 865–876. https://doi.org/10.1177/03611981211020001

Zhao, H.; Feng, S.; Ci, Y.; Xin, M.; Huang, Q. 2022. Scheduling synchronization for overlapping segments in bus lines: speed control and green extension strategies, *Journal of Advanced Transportation* 2022: 2428040. https://doi.org/10.1155/2022/2428040

Zhao, S.; Lu, C.; Liang, S.; Liu, H. 2016. A self-adjusting method to resist bus bunching based on boarding limits, *Mathematical Problems in Engineering* 2016: 8950209. https://doi.org/10.1155/2016/8950209

Zimmermann, L.; Coelho, L. C.; Kraus, W.; Carlson, R. C.; Koehler, L. A. 2021. Bus trajectory optimization with holding, speed and traffic signal actuation in controlled transit systems, *IEEE Access* 9: 143284–143294. https://doi.org/10.1109/access.2021.3122087